

Monoclinic structure of $\text{La}_{1-x}\text{Sr}_x\text{Mn}_z\text{O}_3$ ($x=0.212$, $z=0.958$)R. Tamazyan* and Sander van Smaalen[†]*Laboratory of Crystallography, University of Bayreuth, D-95440, Bayreuth, Germany*

A. Arsenov and Ya. Mukovskii

Moscow State Steel and Alloys Institute, Leninskiy pr.4, 117936 Moscow, Russian Federation

(Received 26 June 2001; revised manuscript received 18 June 2002; published 17 December 2002)

Single-crystal x-ray diffraction is used to show that the crystal structure of $\text{La}_{0.788}\text{Sr}_{0.212}\text{Mn}_{0.958}\text{O}_3$ is monoclinic at room temperature. The Curie temperature of this sample is 324 K. The space group is determined as $I2/c$ with lattice parameters $a=5.4863$ (3) Å, $b=5.5361$ (3) Å, $c=7.7941$ (4) Å, and $\beta=90.74$ (2)°. The crystals are found to be multiply twinned with nonequal volume fractions of the twin domains. A structure refinement against the diffraction data of a twinned crystal converged at $R=0.040$. The structure model involves the same pattern of tiltings of the MnO_6 octahedra as was found in the rhombohedral structure. The principal distortions of the monoclinic structure as compared to the rhombohedral structure are deviations of the O-Mn-O bond angles within the MnO_6 octahedra from 90°. It is argued that the small size of the monoclinic splitting and the very weak additional reflections might not have been visible in neutron diffraction. Our finding of monoclinic symmetry for this compound calls for a revision of the phase diagram of $\text{La}_{1-x}\text{Sr}_x\text{MnO}_3$ compounds ($0 < x < 1$).

DOI: 10.1103/PhysRevB.66.224111

PACS number(s): 75.30.Vn, 61.66.Fn, 61.50.Ks

I. INTRODUCTION

The compounds $\text{La}_{1-x}\text{Sr}_x\text{MnO}_3$ have been studied extensively as one of the classes of compounds in which the colossal magnetoresistance (CMR) effect has been found.^{1,2} Depending on x , they have various properties, including CMR, a metal-insulator transition, different magnetically ordered states, and charge and orbital order.³

The first model explaining CMR was the double-exchange (DE) mechanism.⁴ However, more recent work has shown that CMR as well as the other properties cannot be explained by the DE mechanism alone, and other interactions, like superexchange, are important too.⁵⁻⁷ The charge and spin degrees of freedom interact with both static and dynamic structural distortions,⁸ which need to be taken into account for an explanation of the physical properties of these compounds. With the regular perovskite structure as reference, the modes of distortions involve a Jahn-Teller (JT) distortion of the MnO_6 octahedra and different patterns of tilting of these octahedra. Both distortions are correlated with the valence state of the Mn atoms. Because the principal effect of the substitution of trivalent La by divalent Sr is to oxidize a fraction x of the Mn^{3+} towards Mn^{4+} , the distortions will depend on x . Alternatively, the distortions determine the size of the cavity in which the $\text{La}_{1-x}\text{Sr}_x$ atoms are located, and the distortions thus depend on the average size of $\text{La}_{1-x}\text{Sr}_x$. Again this average size is determined by the value of x . Furthermore, the magnitudes of the magnetic interactions depend on the mode of distortion.

Structure refinements based on x-ray and neutron diffraction data have been used extensively to characterize the phases and phase transitions of CMR compounds.^{9,10} For $\text{La}_{1-x}\text{Sr}_x\text{MnO}_3$ at room temperature three phases have been established.^{3,11} For very small x the structure has orthorhombic symmetry $Pbnm$ with a large JT distortion. This phase has been denoted as O' in the literature. For approximately

$0.1 \leq x \leq 0.16$ the phase O^* is stable, which has the same orthorhombic symmetry as O' , but with a much smaller JT distortion. For $x > 0.16$ the rhombohedral phase R is stable with space group $R\bar{3}c$ and without JT distortions. Again depending on x several phase transitions have been found as a function of temperature.³ Structurally, they have been characterized as transitions between the phases O^* , O' , and R .^{12,13} However, monoclinic and even triclinic phases have been reported too.¹⁴⁻¹⁷ A structure with space group $P2_1/c$ and lattice constants $\sqrt{2}a_c \times \sqrt{2}a_c \times 2a_c$, with $\beta \approx 90.1^\circ$ (a_c being the lattice constant for the ideal, cubic perovskite), has been reported for samples with Sr concentrations in the range $x=0.11-0.125$. The same samples are orthorhombic $Pbnm$ at high temperatures and they become triclinic at low temperatures.¹⁴ A similar monoclinic structure was observed for a sample $\text{La}_{0.85}\text{Ca}_{0.15}\text{MnO}_3$ at room temperature.¹⁵ A monoclinic structure with the same space group $P2_1/c$ but with different lattice constants $2a_c \times 2a_c \times 2a_c$ with $\beta \approx 91^\circ$ has been observed for samples with Sr concentrations $x < 0.1$ that were synthesized at low partial oxygen pressures [$P(\text{O}_2) < 3 \times 10^{-3}$ atm].¹⁶ The third monoclinic structure has been reported to have lattice constants $\sqrt{2}a_c \times \sqrt{2}a_c \times 2a_c$ and $\beta \approx 90.7^\circ$ (no space group is given).¹⁷ It differs from the monoclinic structure reported by Cox *et al.*¹⁴ by the relatively large deviation of the monoclinic angle from 90°.

In addition to the structures listed above, Jirak and co-workers¹⁸ reported a tetragonal structure for $\text{La}_{0.5}\text{Sr}_{0.5}\text{MnO}_3$. Furthermore, superstructures have been reported that would correspond to the formation of charge-ordered states.¹⁹

In the present contribution we report a structural analysis of $\text{La}_{0.788}\text{Sr}_{0.212}\text{Mn}_{0.958}\text{O}_3$ by single-crystal x-ray diffraction. We find that the true symmetry of this compound at room temperature is monoclinic, space group $I2/c$, with lattice constants close to those reported by Mohan *et al.*,¹⁷ and we

report its crystal structure. A detailed comparison is made between this new structure model and the $R\bar{3}c$ structure, which was previously reported for similar compositions. The new possibilities for the structural rearrangements at the phase transitions and their implications for the understanding of the magnetic and electronic properties are discussed.

II. EXPERIMENT

A cylindrical rod of single-crystalline $\text{La}_{0.8}\text{Sr}_{0.2}\text{MnO}_3$ was grown by the floating zone technique with radiation heating.^{20,21} Feed rods were prepared from Mn_3O_4 , SrCO_3 , and La_2O_3 powders, which were mixed in accordance with the desired metal composition $\text{La}_{0.8}\text{Sr}_{0.2}\text{Mn}_{1.0}$. The mixture was milled and subsequently calcinated at 1100°C . The product was milled again, isostatically pressed into cylindrical rods of 6 mm in diameter and 80 mm in length, and then sintered at 1400°C for 24 h to produce the feed rod.

The magnetization of the single crystal was measured between $T=4.2\text{ K}$ and $T=400\text{ K}$ in magnetic fields ranging from 0.05 to 55 kOe. The Curie temperature was determined from the temperature dependence of the magnetization as $T_c=324\text{ K}$.²²

The metals composition was determined by electron microprobe experiments, using a Cameca instrument. Mixed oxides of the metallic elements were used as standards. The ratio $\text{La} : \text{Sr} : \text{Mn} = 0.788(2) : 0.212(1) : 0.963(1)$ was determined by averaging the results of independent measurements at nine different points of the sample.

For the x-ray diffraction experiments several samples of sizes of approximately 0.2 mm were cut off the rod. Diffraction experiments were carried out on a Nonius MACH3 four-circle diffractometer with rotating anode generator, graphite monochromator (Mo $K\alpha$ radiation), and single-point detector. All samples showed multiply splitted Bragg reflections in the x-ray diffraction. One sample with the shape of an almost hexagonal prism was selected for more extensive diffraction experiments.

In first approximation all Bragg reflections could be indexed on an F -centered $2a_c \times 2a_c \times 2a_c$ supercell of the primitive cubic lattice of the perovskite-type structure. Alternative settings for this lattice include a primitive rhombohedral unit cell with $a_r = \sqrt{2}a_c$ and $\alpha_r \approx 60^\circ$, and an I -centered unit cell with lattice parameters $\sqrt{2}a_c \times \sqrt{2}a_c \times 2a_c$ (Fig. 1). Many of the Bragg reflections appeared to be split, indicating that the true lattice symmetry is lower than rhombohedral and that the crystal is twinned. In order to characterize the twinning the diffracted intensities of a few selected reflections were measured in dependence on the crystal orientation (ω and χ angles) and on the diffraction angle (2θ). Figure 2(a) gives the intensity of the $(110)_c$ reflection as a function of ω and θ [the indices $(hkl)_c$ refer to the primitive cubic cell]. It is clearly seen that there are four maxima occurring at different scattering angles and different orientations of the crystal. Multiple maxima (splitted reflections) have also been observed for the $(100)_c$ and $(111)_c$ reflections (Fig. 2).

Any symmetry operator of the cubic point group $m\bar{3}m$ of the perovskite structure type that does not correspond to a

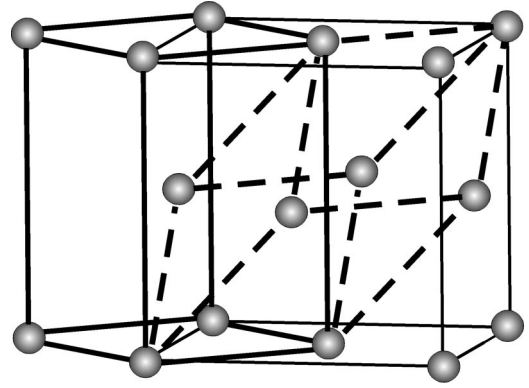


FIG. 1. The lattice of $\text{La}_{0.788}\text{Sr}_{0.212}\text{Mn}_{0.958}\text{O}_3$ with the F -centered (thin lines), I -centered (thick lines), and primitive-rhombohedral (dashed lines) unit cells indicated.

symmetry operator of the structure may become a twinning operator. Taking into account the lattice symmetry this allows us to compute the expected splittings of the reflections for each possible space group of the low-symmetry phase (Table I). The comparison with the observed splittings shows that the true lattice symmetry of the investigated crystal is C -centered monoclinic. An equivalent description is obtained with the I -centered $\sqrt{2}a_c \times \sqrt{2}a_c \times 2a_c$ unit cell that we will adopt here.

Assuming the monoclinic symmetry to be a subgroup of $R\bar{3}c$ leads to the space group $I2/c$. This space group was confirmed by the structure refinements. Further evidence for the monoclinic symmetry was obtained from the complete data collections (see below).

Previously, the space group $R\bar{3}c$ was proposed as the symmetry for this phase. We have observed 34 weak reflections violating the extinction conditions implied by the glide planes in $R\bar{3}c$. These intensities remained when the x-ray diffraction was measured with a reduced voltage of the x-ray tube. This showed that these reflections were not due to diffraction of $\lambda/2$ radiation, contrary to intensities observed at positions violating the F centering, which disappeared on reducing the voltage. Another origin for these weak reflections might be multiple scattering. Therefore Ψ scans (scattered intensity as a function of the azimuthal angle Ψ) were made for several of these reflections. Figure 3(a) clearly shows that the $(\bar{1}\bar{1}1)_R$ reflection, violating the extinction rules of $R\bar{3}c$, is present for all values of Ψ , and that this reflection is not due to multiple scattering. (The subscript R indicates the indexing with respect to the primitive rhombohedral lattice; see Fig. 1.) Figure 3(b) shows the dependence on Ψ of the intensity of the reflection $(1\bar{1}0)_R$, which is an allowed reflection in space group $R\bar{3}c$. The observed variations of intensities with Ψ are almost equal for both reflections. This strongly suggests that variations in absorption are responsible for the variations in the intensities with Ψ . Thus we have observed 34 reflections that violate the extinction conditions of the space group $R\bar{3}c$. They can all be explained by one of the orientations of a monoclinic structure with space group $I2/c$.

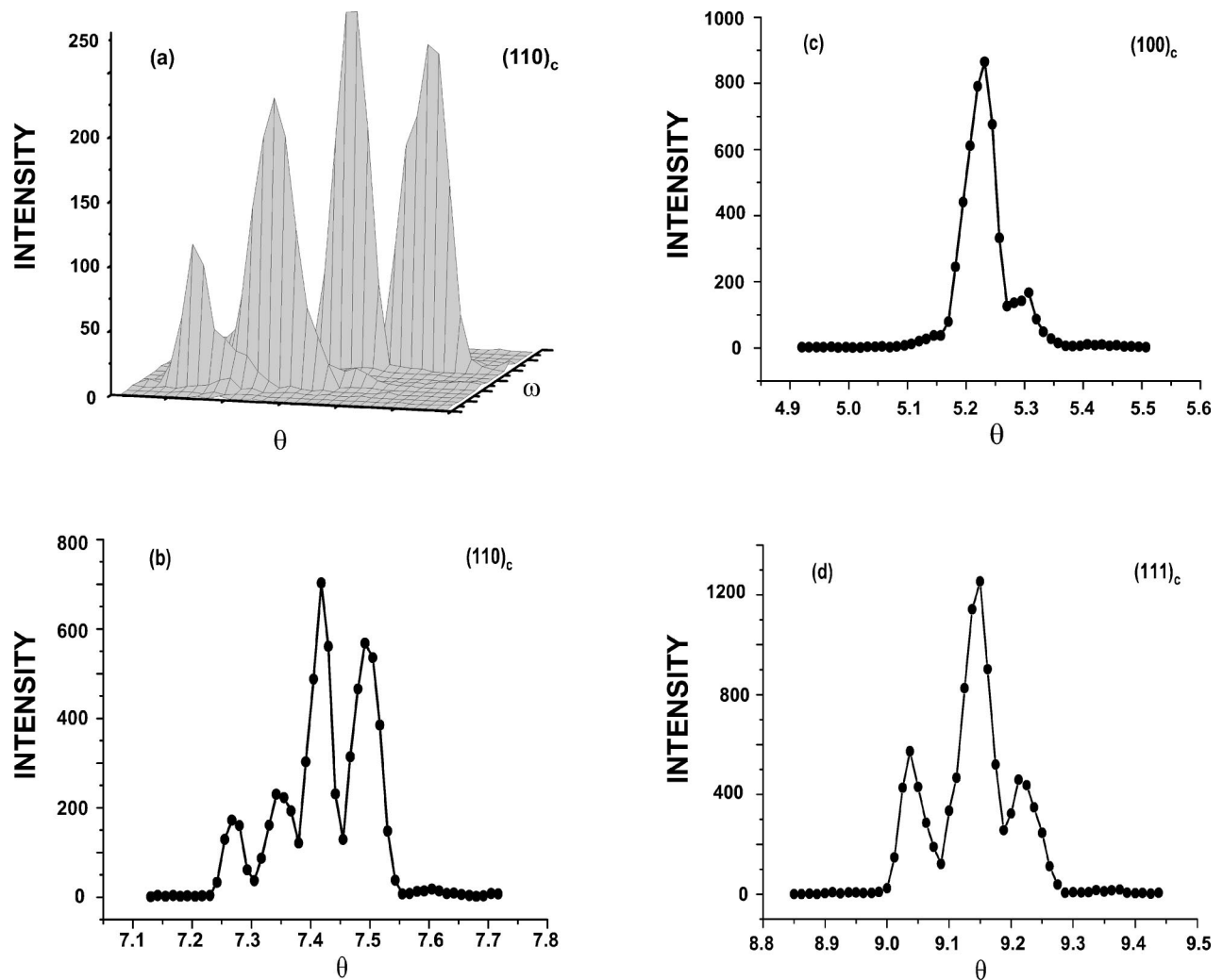


FIG. 2. Reflection profiles as a function of half of the scattering angle (θ) and of the crystal orientation (ω). (a) ω - θ section of the $(110)_c$ reflection, (b) projection onto θ of the scattered intensity around the $(110)_c$ reflection, (c) around $(100)_c$, and (d) around $(111)_c$.

Integrated intensities were measured for all Bragg reflections in a half sphere with $\sin(\theta)/\lambda \leq 1.0$. A large detector window was selected, in order to measure the sum of intensities of the components of each split Bragg reflection. The

data reduction with usual corrections was made using the computer program HELENA,²³ and the absorption correction ($\mu = 23.79 \text{ mm}^{-1}$) was made with aid of the computer program HABITUS.²⁴ A total of 2047 reflections were measured,

TABLE I. Splitting of Bragg reflections in 2θ (the scattering angle) for the $(100)_c$, $(110)_c$, and $(111)_c$ reflections. The expected numbers of split components are given for various symmetries of the low-symmetry phases.

Point group	Lattice type	Number of twin domains	Number of different 2θ values		
			$(100)_c$	$(110)_c$	$(111)_c$
$\bar{1}$	P	24	3	6	4
$2/m$	P	12	3	4	2
$2/m$	C	12	2	4	3
mmm	P	6	3	3	1
mmm	C	6	2	3	2
$4/mmm$	P	3	2	2	1
$\bar{3}m$	R	4	1	2	2
Present experiment on $\text{La}_{0.788}\text{Sr}_{0.212}\text{Mn}_{0.958}\text{O}_3$			2	4	3

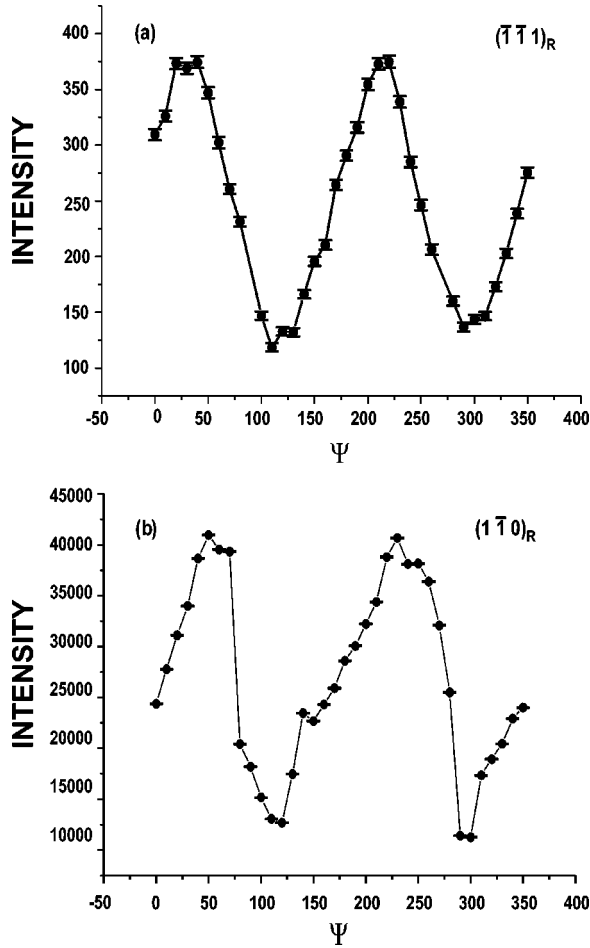


FIG. 3. Intensities of (a) the $(\bar{1}\bar{1}\bar{1})_R$ reflection and (b) the $(1\bar{1}0)_R$ reflection as a function of the crystal orientation (Ψ angle). Note that the $(\bar{1}\bar{1}\bar{1})_R$ reflection violates the extinction rules of the space group $R\bar{3}c$, while the $(1\bar{1}0)_R$ is allowed within $R\bar{3}c$.

of which there were 1320 observed reflections with $I \geq 3\sigma(I)$. Because different volume fractions were found for the 12 possible twin domains, the diffraction symmetry was only $\bar{1}$.²⁵ This symmetry was used for averaging the reflection intensities, resulting in 1249 unique observed reflections that were used in the refinements. The internal R_I factor, describing the disagreement of measured intensities for symmetry-equivalent reflections, was $R_I=0.049$. Alternatively, averaging the reflections in $\bar{3}m$ leads to 266 unique observed reflections with $R_I=0.088$. The crystallographic data are summarized in Table II.

III. STRUCTURE REFINEMENTS

The diffraction data can be reasonably well fitted with a structure model in $R\bar{3}c$ symmetry. The refinement converged at $R=0.059$ for the data averaged in $\bar{1}$ symmetry, and it converged at $R=0.025$ for the data averaged in $\bar{3}m$ symmetry. The apparently good fit can be explained by the fact that the monoclinic structure can be described as a relatively small distortion from the rhombohedral structure and by the

TABLE II. Experimental data. Standard deviations are given in parentheses.

Temperature (K)	300
a (\AA)	5.4863 (3)
b (\AA)	5.5361 (3)
c (\AA)	7.7941 (4)
β (deg.)	90.74 (2)
V (\AA^3)	236.7
Space group	$I2/c$
$\rho_{\text{calc.}}$ (g/cm^3)	6.496
Number of measured reflections	2047
Number of observed reflections	1320
Number of unique reflections	1249
Refinement	
Number of parameters	32
R	0.040
wR	0.048
Twin volume fraction 1	0.595
Twin volume fraction 2	0.068 (7)
Twin volume fraction 3	0.039 (7)
Twin volume fraction 4	0.177 (1)
Twin volume fraction 5	0.121 (4)
Occupation Mn-site (z)	0.958 (8)
Occupation La-site (y)	0.998 (7)
Composition	$\text{La}_{0.788}\text{Sr}_{0.212}\text{Mn}_{0.958}\text{O}_3$

fact that the measured intensities are the sum of intensities from different twin domains, thus averaging out the effect of the lower point symmetry. Nevertheless, our observation of scattered intensities at points forbidden by the $R\bar{3}c$ space group and our observation of split Bragg reflections definitely showed that the true symmetry of our sample was monoclinic. All structure refinements were performed with JANA2000.²⁶

Refinements of a structure model with monoclinic symmetry $I2/c$ were performed starting from the rhombohedral structure. The measured integrated intensities of the Bragg reflections were considered to be sum of intensities of Bragg reflections of the various twin domains. The refinement converged to a fit with $R=0.040$. It was found that only 5 out of the 12 possible twin domains did have significant volume fractions.

It is known that the oxygen content might deviate from the nominal composition and that it depends on the precise circumstances of the crystal growth. Usually up to a few percent of excess of oxygen is found, and the chemical composition can be represented by $\text{La}_{1-x}\text{Sr}_x\text{MnO}_{3+\delta}$ with $\delta \ll 1$.¹⁶ Structurally, the excess of oxygen is accommodated by fully occupied oxygen sites and vacancies on the La and Mn sublattices.^{27,28} Then, the composition can be described as $(\text{La}_{1-x}\text{Sr}_x)_y\text{Mn}_z\text{O}_3$. Because intensities of Bragg reflections in x-ray diffraction are only sensitive to the total number of electrons on each site, the parameters x and y are correlated and they cannot be varied simultaneously. Therefore, we fixed the value of $x=0.212$ towards the value obtained from the microprobe experiment. Structure refine-

TABLE III. Atomic coordinates (relative to the cell axes) and equivalent isotropic temperature parameters U_{eq} (\AA^2) obtained from the final refinement.

Atom	x	y	z	U_{eq}
Mn	0	0	0	0.0039 (2)
La/Sr	$\frac{1}{2}$	0.0003 (1)	$\frac{1}{4}$	0.0071 (1)
O1	$\frac{1}{2}$	0.550 (1)	$\frac{3}{4}$	0.012 (1)
O2	0.2249 (7)	0.2759 (8)	0.5253(5)	0.011 (1)

ments were performed including the variation of the site occupancies y and z . The result shows that the La site is fully occupied and that the Mn site contains vacancies (Table II). The composition as obtained from the refinement is in good agreement with the values determined by the microprobe experiment. The structure parameters corresponding to the best fit are summarized in Tables II and III.

IV. DISCUSSION

The crystal structures of $(\text{La}_{1-x}\text{Sr}_x)_y\text{Mn}_z\text{O}_3$ manganites can be described as distorted perovskite ABO_3 type structures ($A = \text{La}_{1-x}\text{Sr}_x$). The A cations occupy cavities of the three-dimensional (3D) network of vertex sharing BO_6 octahedra. The size of the cavity in the undistorted perovskite structure depends on the B-O bond length. Tilting of the BO_6 octahedra modifies the size of the cavity available for the A-type cation. It is well known that A-type cations of various sizes are accommodated in the structure by different magnitudes of tilting of the MnO_6 octahedra. Different patterns of tilting correspond to different superstructures of the cubic perovskite structure type,²⁹ including the $R\bar{3}c$ and $Pbnm$ structures as have been reported for $\text{La}_{1-x}\text{Sr}_x\text{MnO}_3$.¹⁶ For the monoclinic structure presented here we find that the pattern of tilting is similar to that of the rhombohedral structure reported previously (Fig. 4). It is described by a rotation of the MnO_6 octahedral groups approximately about the $[111]_c$ direction over 17° .

A second type of distortion that has been observed in rare earth manganites is the JT distortion of the MnO_6 octahedral groups. It stabilizes the Mn^{3+} oxidation state, and it is expected to be zero for Mn^{4+} . Structurally, the JT distortion is characterized by two long and four short Mn-O bonds.¹⁶ In pure LaMnO_3 all Mn atoms are in Mn^{3+} state. In $(\text{La}_{1-x}\text{Sr}_x)_y\text{Mn}_z\text{O}_3$ compounds both replacement of La^{3+} by Sr^{2+} (x) and cation site vacancies (y and z) create Mn^{4+} on Mn sites. In this way each of the parameters x , y , and z will influence the crystal structure, including the Mn-O bond lengths, JT distortions, and tilting schemes of the MnO_6 octahedral groups.

For the rhombohedral structures the coherent JT distortion is zero as determined by symmetry. The monoclinic $I2/c$ symmetry allows a JT distortion, but we find that all Mn-O bonds have approximately equal lengths (Table IV). This result establishes that there is at most a very small coherent JT distortion in $\text{La}_{0.788}\text{Sr}_{0.212}\text{Mn}_{0.958}\text{O}_3$ at room temperature. The temperature factors of the oxygen atoms are anisotropic

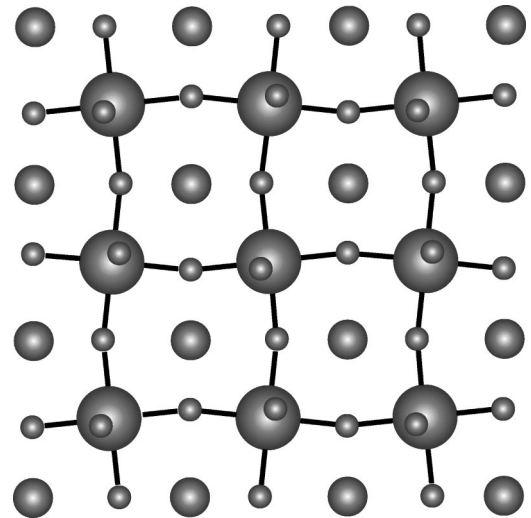


FIG. 4. Projection of the monoclinic structure of $\text{La}_{0.788}\text{Sr}_{0.212}\text{Mn}_{0.958}\text{O}_3$ along (001) [corresponds to $(00\frac{1}{2})_c$]. Large circles represent Mn, small circles represent O, and medium-sized circles represent La/Sr. Mn-O bonds are shown as sticks.

with much smaller values in the directions of the Mn-O bonds than perpendicular to them (Fig. 5). This suggests the absence of large incoherent JT distortions as well.⁵ The near absence of JT distortions can be explained by the high fraction of Mn^{4+} ions that exist due to vacancies on the Mn site. It is noticed that $I2/c$ was determined as the space group for $\text{Pr}_{0.6}\text{Sr}_{0.4}\text{MnO}_3$ too.³⁰

Previous investigations on compounds with similar compositions have found them to be in the ferromagnetic state at room temperature. For these compounds rhombohedral symmetry was reported with only small incoherent JT distortions.³ Presently, we find similar properties for $\text{La}_{0.788}\text{Sr}_{0.212}\text{Mn}_{0.958}\text{O}_3$, albeit with a different symmetry of the structure. Apart from an, at most, very small coherent JT distortion, the monoclinic structure is distinguished from the rhombohedral structure by further distortions of the MnO_6

TABLE IV. Interatomic distances (\AA) and bond angles (degrees) for the final structure model. The number of equivalent bonds of each type is given in square brackets.

Atoms	Value
Mn - O1 [2]	1.9681 (8)
Mn - O2 [2]	1.966 (3)
Mn - O2 [2]	1.972 (4)
Mn - O1 - Mn	163.8 (3)
Mn - O2 - Mn	163.6 (2)
La/Sr - O1 [2]	2.7569 (5)
La/Sr - O1	2.490 (5)
La/Sr - O1	3.047 (5)
La/Sr - O2 [2]	2.488 (3)
La/Sr - O2 [2]	2.760 (3)
La/Sr - O2 [2]	2.756 (3)
La/Sr - O2 [2]	3.049 (3)

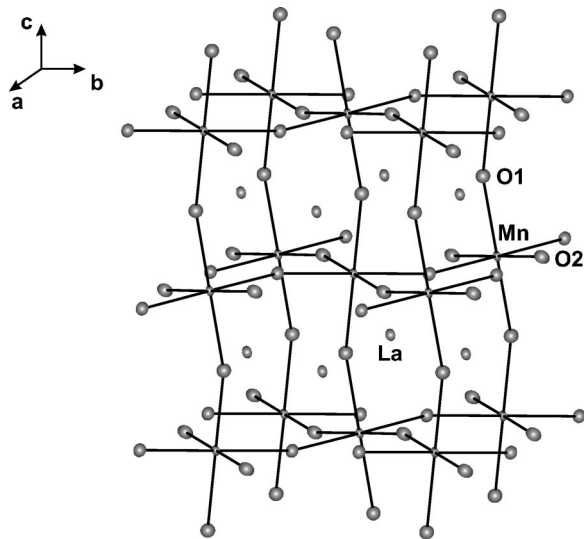


FIG. 5. Perspective view of the monoclinic crystal structure of $\text{La}_{0.788}\text{Sr}_{0.212}\text{Mn}_{0.958}\text{O}_3$. Thermal ellipsoids are drawn for all atoms.

octahedral groups. This is exemplified by deviations of the O-Mn-O bond angles from 90° , with values between 88.97° and 88.83° in the $I2/c$ structure. (The three O-Mn-O angles of 180° retain this value exactly because of the symmetry.) It is likely that these small distortions do influence the state of the manganese ions and thus indirectly influence the magnetic coupling in the structure.

We have determined that $\text{La}_{0.788}\text{Sr}_{0.212}\text{Mn}_{0.958}\text{O}_3$ has a monoclinic $I2/c$ structure at room temperature. A monoclinic lattice has been reported previously for this composition, but without giving the space group or structure model.¹⁷ The $I2/c$ monoclinic structure differs from the rhombohedral structure model by small distortions only. The monoclinic structure reported for $\text{La}_{1-x}\text{Sr}_x\text{MnO}_{3+\delta}$ with $x < 0.15$ has a different lattice and different symmetry (space group $P2_1/c$),¹⁴⁻¹⁶ and obviously is not directly related to the present structure.

V. CONCLUSIONS

We have established that $\text{La}_{0.788}\text{Sr}_{0.212}\text{Mn}_{0.958}\text{O}_3$ has monoclinic $I2/c$ symmetry in its ferromagnetic state at room temperature. The space group $I2/c$ is a subgroup of $R\bar{3}c$, and the monoclinic crystal structure represents a small but definite distortion away from the rhombohedral structure that was previously reported for similar compositions. On the other hand, the low-temperature, orthorhombic structure cor-

responds to an essentially different pattern of tiltings than the rhombohedral structure.¹⁶ The phase transition that occurs below room temperature has been described previously as a transition from $R\bar{3}c$ towards $Pbnm$ symmetry. If true, it would correspond to a sudden rearrangement of the pattern of tiltings of the MnO_6 octahedra. The $I2/c$ monoclinic symmetry provides for an alternative interpretation of the phase transitions as continuous structural transitions. A possible high-temperature transition would be between phases with rhombohedral and monoclinic symmetries, respectively. Because $I2/c$ is a subgroup of $R\bar{3}c$, this can be a continuous transition. The low-temperature transition would be between phases with symmetries $I2/c$ and $Pbnm$, respectively. There is no subgroup-supergroup relation, but the pattern of tilts can be changed continuously going from one symmetry to the other. An intermediate monoclinic structure was also observed between the rhombohedral and tetragonal phases of $\text{PbZr}_{1-x}\text{Ti}_x\text{O}_3$.³¹

It might be the case that the symmetry of $(\text{La}_{1-x}\text{Sr}_x)_y\text{Mn}_z\text{O}_3$ will depend not only on the doping (the parameter x) but also on the oxygen content or on the vacancies at the cation sites (the parameters y and z). However, the $I2/c$ monoclinic symmetry has not been reported before for any composition of the (La,Sr) manganites. We consider it unlikely that compositions similar to the composition of the present single crystal would not have been studied before. On the other hand, the relatively small sizes of the splittings of the Bragg reflections might have been easily overlooked in previous experiments. In the case of neutron diffraction or x-ray powder diffraction using a standard laboratory diffractometer, the widths of the peaks might be larger than the splittings, and it would have been impossible to observe splittings of sizes similar to the ones reported here. The good fit to the intensity data by a structure model with $R\bar{3}c$ symmetry will not have given any incentive to search for structures with lower symmetries. Of course, the fit of the intensity data in $R\bar{3}c$ disregards the splittings of the reflections as presently observed. These splittings and the observed (weak) intensities at positions forbidden by $R\bar{3}c$ provide conclusive evidence for the monoclinic symmetry of the present single crystal. We think that the phase diagram of $\text{La}_{1-x}\text{Sr}_x\text{MnO}_3$ needs to be reconsidered, taking into account the $I2/c$ monoclinic symmetry.

ACKNOWLEDGMENT

Financial support by the German Science Foundation (DFG) is gratefully acknowledged.

*Permanent address: Molecule Structure Research Center National Academy of Sciences RA, Azatutyan 26, 375014 Yerevan, Republic of Armenia. Electronic address: rafael@msrc.am

†Correspondence author. Electronic address: smash@uni-bayreuth.de

¹G. H. Jonker and J. H. van Santen, *Physica (Amsterdam)* **16**, 337 (1950).

²J. H. van Santen and G. H. Jonker, *Physica (Amsterdam)* **16**, 599

(1950).

³B. Dabrowski, X. Xiong, Z. Bukowski, R. Dybziński, P. W. Klamm, J. E. Siewenie, O. Chmaissem, J. Schaffer, C. W. Kimball, J. D. Jorgensen, and S. Short, *Phys. Rev. B* **60**, 7006 (1999).

⁴C. Zener, *Phys. Rev.* **82**, 403 (1951).

⁵A. J. Millis, P. B. Littlewood, and B. I. Shraiman, *Phys. Rev. Lett.* **74**, 5144 (1995).

⁶A. J. Millis, *J. Appl. Phys.* **81**, 5502 (1997).

- ⁷J. B. Goodenough, *J. Appl. Phys.* **81**, 5330 (1997).
- ⁸J. S. Zhou and J. B. Goodenough, *Phys. Rev. B* **64**, 024421 (2001).
- ⁹Y. Tokura and Y. Tomioka, *J. Magn. Magn. Mater.* **200**, 1 (1999).
- ¹⁰A. P. Ramirez, *J. Phys.: Condens. Matter* **9**, 8171 (1997).
- ¹¹A. Urushibara, Y. Moritomo, T. Arima, A. Asamitsu, G. Kido, and Y. Tokura, *Phys. Rev. B* **51**, 14 103 (1995).
- ¹²H. Kawano, R. Kajimoto, M. Kubota, and H. Yoshizawa, *Phys. Rev. B* **53**, 14 709 (1996).
- ¹³L. Pinsard, J. Rodriguez-Carvajal, and A. Revcolevschi, *J. Alloys Compd.* **262-263**, 152 (1997).
- ¹⁴D. E. Cox, T. Iglesias, E. Moshopoulou, K. Hirota, K. Takahashi, and Y. Endoh, *Phys. Rev. B* **64**, 024431 (2001).
- ¹⁵M. V. Lobanov, A. M. Balagurov, V. J. Pomjakushin, P. Fischer, M. Gutmann, A. M. Abakumov, O. G. D'yachenko, E. V. Antipov, O. I. Lebedev, and G. van Tendeloo, *Phys. Rev. B* **61**, 8941 (2000).
- ¹⁶J. F. Mitchell, D. N. Argyriou, C. D. Potter, D. G. Hinks, J. D. Jorgensen, and S. D. Bader, *Phys. Rev. B* **54**, 6172 (1996).
- ¹⁷C. V. Mohan, M. Seeger, H. Kronmuller, P. Murugaraj, and J. Maier, *J. Magn. Magn. Mater.* **183**, 348 (1998).
- ¹⁸Z. Jirak, J. Hejtmanek, K. Knizek, V. S. M. Marysko, and R. Sonntag, *J. Magn. Magn. Mater.* **217**, 113 (2000).
- ¹⁹Y. Yamada, J. Suzuki, K. Oikawa, S. Katano, and J. A. Fernandez-Baca, *Phys. Rev. B* **62**, 11 600 (2000).
- ²⁰D. Shulyatev, S. Karabashev, A. Arsenov, and Y. Mukovskii, *J. Cryst. Growth* **198/199**, 511 (1999).
- ²¹A. M. Balabashov, S. G. Karabashev, Y. M. Mukovskii, and S. A. Zverkov, *J. Cryst. Growth* **16**, 36 (1996).
- ²²V. E. Arkhipov, V. P. Dyakina, S. G. Karabashev, V. V. Marchenkov, Y. M. Mukovskii, V. E. Naish, V. E. Startsev, E. P. Khlybov, and A. Chopnik, *Phys. Met. Metallogr.* **84**, 632 (1997).
- ²³A. Meetsma and T. Spek, computer program HELENA, University of Groningen, 2000.
- ²⁴W. Herrendorf, Ph.D. thesis, University of Karlsruhe, 1993.
- ²⁵R. Tamazyan, Y. Malinovskii, and V. Simonov, *Bull. Soc. Cat. Cien.* **12**, 221 (1991).
- ²⁶V. Petricek and M. Dusek, computer program JANA2000, Institute of Physics of the Academy of Sciences, Praha, Czech Republic, 2000.
- ²⁷J. A. M. van Roosmalen, E. H. P. Cordfunke, R. B. Helmholdt, and H. W. Zandbergen, *J. Solid State Chem.* **110**, 100 (1994).
- ²⁸J. A. M. van Roosmalen and E. H. P. Cordfunke, *J. Solid State Chem.* **110**, 106 (1994).
- ²⁹A. M. Glazer, *Acta Crystallogr., Sect. B: Struct. Crystallogr. Cryst. Chem.* **28**, 3384 (1972).
- ³⁰C. Ritter, P. G. Radaelli, M. R. Lees, J. Barrat, G. Balakrishnan, and D. M. Paul, *J. Solid State Chem.* **127**, 276 (1996).
- ³¹B. Noheda, D. E. Cox, G. Shirane, R. Guo, B. Jones, and L. E. Cross, *Phys. Rev. B* **63**, 014103 (2000).